ELSEVIER

Journal of Computational and Applied Mathematics 131 (2001) 381–405

JOURNAL OF COMPUTATIONAL AND APPLIED MATHEMATICS

www.elsevier.nl/locate/cam

On a uniformly accurate finite difference approximation of a singularly perturbed reaction–diffusion problem using grid equidistribution

G. Beckett *, J.A. Mackenzie

Department of Mathematics, University of Strathclyde, Livingstone Tower, 26 Richmond Street, Glasgow, Scotland G1 1XH, UK

Received 29 April 1999; received in revised form 13 December 1999

Abstract

We examine the convergence properties of a finite difference approximation of a singularly perturbed reaction–diffusion boundary value problem using a nonuniform grid. The grid is based on the equidistribution of a positive monitor function that is a linear combination of a constant floor and a power of the second derivative of the solution. Analysis shows how the monitor function can be chosen to ensure that the accuracy of the numerical approximation is insensitive to the size of the singular perturbation parameter. The use of equidistribution principles appears in many practical grid adaption schemes and our analysis provides insight into the convergence behaviour on such grids. Numerical results are given that confirm the uniform convergence rates. © 2001 Elsevier Science B.V. All rights reserved.

Keywords: Uniform convergence; Adaptivity; Equidistribution; Singular perturbation; Reaction–diffusion

1. Introduction

This paper is concerned with the numerical solution of the model boundary value problem

$$Lu = -\varepsilon u''(x) + b(x)u(x) = f(x), \quad x \in (0,1),$$

$$u(0) = 0, \quad u(1) = 0. \tag{1}$$

where $b(x) \geqslant \beta > 0$ and $b(x), f(x)$ are assumed to be sufficiently smooth. In particular, we are interested in the singularly perturbed regime where $0 < \varepsilon \ll \beta$.

It is well known that (1) is difficult to solve efficiently using standard numerical techniques due to the possibility of steep exponential boundary layers. Such layers are also present in more general

* Corresponding author.

E-mail address: g.beckett@maths.strath.ac.uk (G. Beckett).

PII: S0377-0427(00)00260-0

singularly perturbed reaction–diffusion problems. Ideally, we would like the accuracy of a numerical solution of (1) to be insensitive to the size of ε. This has led to the development of uniformly accurate methods. A numerical method is said to be uniformly pth-order convergent if, on a grid with N intervals, the error is such that

$$\max_{0 \leqslant j \leqslant N} |u(x_j) - u_j| < CN^{-p}, \tag{2}$$

where the constant C is independent of N and the singular perturbation parameter, ε. Such a property is clearly desirable as it shows that the method converges satisfactorily even for very small values of ε. There are two common strategies for constructing uniformly convergent methods. The first is to implement a discretisation that explicitly uses the fact that the solution of (1) is exponential in nature. Many such exponentially fitted methods have been proposed including those of Doolan et al. [12], O'Riordan and Stynes [21] and Roos [27]. These methods aim to produce accurate solutions even on relatively coarse grids. However, they can be computationally expensive to implement, especially for nonlinear problems, and are not easily extendible to multi-dimensions. The second strategy is to use a relatively simple discretisation on a suitable nonuniform grid. If a priori information is available about the exact solution, then highly appropriate grids can be generated. The grids proposed by Bakhvalov [3], Vulanović [30], and Gartland [14] are exponentially stretched within the boundary layers and are uniform external to the layers. Simpler piecewise-uniform grids have been proposed by Shishkin [29] (also see [19] and Section 3.2 below). Using these grids, various discretisations have been shown to be uniformly convergent. However, the successful application of all of the approaches above requires a significant amount of a priori information about the presence, location, and thickness of any layers.

A more flexible strategy is to generate an appropriate nonuniform grid using the numerical solution. A solution-adaptive algorithm attempts to detect automatically the location, height and thickness of any boundary layers thus obviating the need to provide this information a priori.

A commonly used technique for determining the grid points is to use an equidistribution principle. This can be thought of as giving rise to a mapping, $x = x(\xi)$, relating a computational coordinate $\xi \in [0,1]$ to the physical coordinate $x \in [0,1]$, defined by

$$\int_0^{x(\xi)} M(u(s),s)\,\mathrm{d}s = \xi \int_0^1 M(u(s),s)\,\mathrm{d}s,$$

where $M(u(x),x) > 0$ is a suitable monitor function. Adaptive methods based on mesh equidistribution have been successfully used to solve one-dimensional boundary value problems (see, for example, [11,22,28,31]) and the idea of equidistribution can also be extended to the adaptive generation of quadrilateral grids in two dimensions [15,17]. Mesh equidistribution has also been used to adapt the spatial grid for time-dependent problems [5,16,20].

Although algorithms based on equidistribution principles have been applied to a wide range of practical problems, very little theoretical analysis has been carried out to explain their success. This is primarily due to the inherent nonlinear nature of adaptive methods. The error analysis in Pereyra and Sewell [22] and Ascher et al. [1] is based on an asymptotic expansion of the local truncation error where only the lowest order terms are retained. A much more careful analysis is needed to establish a uniform error bound of the form (2). Recently, Qiu and Sloan [24], Qiu et al. [25], and Mackenzie [18] have analysed upwind methods for the solution of homogeneous convection–

diffusion problems using grids based on equidistribution of $M = |u'|^{1/m}$, where $m \geqslant 2$. On these grids it is shown that uniform convergence can be obtained.

However, for inhomogeneous problems a drawback with adapting purely on the basis of the solution gradient is that the vast majority of the mesh points lie within the boundary layer. For these problems, Beckett and Mackenzie [4] consider a decomposition of the analytic solution into a smooth component, $v(x)$, and a layer component, $w(x)$, such that $u(x) = v(x) + w(x)$. Since the main numerical difficulty is the presence of a steep boundary layer, they consider the monitor function

$$M = \alpha + |w''(x)|^{1/m}, \quad m > 0,$$

where α is a positive constant that is independent of N, chosen to prevent mesh starvation and to improve the robustness of the adaptive grid procedure, see [23]. Often the floor is chosen in an ad hoc way. However, Beckett and Mackenzie [4] show how to choose it to ensure uniform convergence.

The main aim of this paper is to apply the approach of [4] to singularly perturbed reaction–diffusion problems using the same monitor function. Depending on the form of $v(x)$, these problems may have one or two boundary layers. In addition, when two layers are present they may be of different thickness and steepness. We will show how equidistribution of M results in a grid that can accommodate all of these cases. The analysis of [4] proves first-order convergence of simple upwind methods for convection–diffusion problems. To establish second-order convergence of the central difference approximation to (1), it is necessary to derive additional smoothness properties of the grid within the layer region. Furthermore, we show that super-convergence at the grid nodes can be obtained for a constant coefficient problem when $m = 4$.

Asymptotically, we would like to establish that $u_j \to u(x_j)$ and $x_j \to x(\xi_j)$. This fully discretised system is nonlinear even for a linear boundary value problem. This is the main reason for the lack of convergence analysis of adaptive grid methods. To initiate analysis, we will linearise the problem by making the assumption that the grid exactly equidistributes M where $w(x)$ is given by the leading term of its asymptotic expansion. Of course, the locations of the grid points of a truly adaptive method will differ slightly from those using this assumption. In Section 5, we present numerical results showing that these discrepancies do not affect the uniform convergence predicted.

The layout of the rest of this paper is as follows. In Section 2 we derive the decomposition using techniques similar to those of Dobrowolski and Roos [10]. Then, in Section 3 we outline the numerical discretisation of (1) and describe the generation of the equidistributing grid. Properties of the grid that are crucial to the error analysis are also derived in this section. The error analysis is carried out in Section 4: a second-order uniformly accurate error bound is derived in the l_∞ norm, and via piecewise linear interpolation of the discrete solution, the bound is extended to the stronger L_∞ norm. In the final section, we present numerical results that confirm the validity of the derived error estimates. In an appendix we show that super-convergence can be obtained for certain problems.

Throughout the paper, C will denote a generic constant that is independent of N and ε, and that can take different values at different places, even in the same argument.

2. Solution decomposition

It is well known that the solution to (1) exhibits boundary layer behaviour. The following two lemmas give a very useful decomposition of the exact solution which isolates these layers.

Lemma 1. *For any prescribed order, r, the solution $u(x)$ of (1) is such that*

$$|u^{(p)}(x)| < C(1+\varepsilon^{-p/2})e(x,\beta), \quad p=0,\dots,r,$$

where $e(x,\beta) = \mathrm{e}^{-\sqrt{(\beta/\varepsilon)}x} + \mathrm{e}^{-\sqrt{(\beta/\varepsilon)}(1-x)}$.

Proof. See [19] for a proof when $r=3$. The argument presented there can be extended to arbitrary r.

Lemma 2. *The solution $u(x)$ of (1) has the form*

$$u(x) = v(x) + w(x),$$

where the smooth component $v(x)$ satisfies

$$Lv(x) = f(x), \quad x \in (0,1),$$

$$v(0) = -w(0), \quad v(1) = -w(1)$$

and the singular component satisfies

$$Lw(x) = 0, \quad x \in (0,1),$$

$$w(0) = -v(0), \quad w(1) = -v(1).$$

Furthermore, for arbitrary k and $0 \leqslant p \leqslant 2k+1$, the following bounds hold:

$$|v^{(p)}(x)| < C \tag{3}$$

and

$$|w^{(p)}(x)| < C\varepsilon^{-p/2}(\mathrm{e}^{-\sqrt{(b(0)/\varepsilon)}x} + \mathrm{e}^{-\sqrt{(b(1)/\varepsilon)}(1-x)}). \tag{4}$$

Proof. Define

$$v(x) = \sum_{l=0}^{2k+1} \varepsilon^{l/2} v_l(x) + \varepsilon^{k+1} v^*_{2(k+1)}(x).$$

Then, substituting $v(x)$ into (1) and equating powers of ε, we see immediately that the odd terms of the expansion are identically zero, and the even terms satisfy

$$L_0 v_0(x) = f(x),$$

$$L_0 v_{2l}(x) = -L_1 v_{2(l-1)}(x), \quad l = 1,\dots,k,$$

$$Lv^*_{2(k+1)}(x) = -L_1 v_{2k}(x), \quad v^*_{2(k+1)}(0) = v^*_{2(k+1)}(1) = 0,$$

where $L_0 = b(x)I$ and $L_1 = -\mathrm{d}^2/\mathrm{d}x^2$. Then, using Lemma 1, one can see immediately that

$$|v^{(p)}(x)| < C \quad \text{for } p = 0, \ldots, 2k+1.$$

The component $v(x)$ satisfies the differential equation (1) but not the boundary conditions. To rectify this, we introduce the singular component $w(x) = w^-(x) + w^+(x)$, where

$$w^-(x) = \sum_{l=0}^{2k+1} \varepsilon^{l/2} w_l^-(x) + \varepsilon^{k+1} w_{2(k+1)}^{*-}(x) \tag{5}$$

and

$$w^+(x) = \sum_{l=0}^{2k+1} \varepsilon^{l/2} w_l^+(x) + \varepsilon^{k+1} w_{2(k+1)}^{*+}(x). \tag{6}$$

For the left-hand boundary layer, we introduce the coordinate transformation $\xi = x/\sqrt{\varepsilon}$ and define

$$\hat{L} = -\frac{\mathrm{d}^2}{\mathrm{d}\xi^2} + b(0)I.$$

Considering a Taylor series expansion of $b(\sqrt{\varepsilon}\xi)$, we see that $w_l^-(\xi)$ satisfies

$$\hat{L} w_0^-(\xi) = 0,$$

$$w_0^-(0) = -v_0(0), \quad \lim_{\xi\to\infty} (w_0^-(\xi)) = 0,$$

$$\hat{L} w_l^-(\xi) = -\hat{L}^*(w_0^-, \ldots, w_{l-1}^-)(\xi),$$

$$w_l^-(0) = -v_l(0), \quad \lim_{\xi\to\infty} (w_l^-(\xi)) = 0, \quad l = 1, \ldots, 2k+1$$

and

$$L w_{2(k+1)}^{*-}(x) = -\varepsilon^{-(k+1)} L(w_0^- + \cdots + \varepsilon^{(2k+1)/2} w_{2k+1}^-)(x),$$

$$w_{2(k+1)}^{*-}(0) = 0, \quad w_{2(k+1)}^{*-}(1) = -\varepsilon^{-(k+1)}(w_0^- + \cdots + \varepsilon^{(2k+1)/2} w_{2k+1}^-)(1),$$

where

$$\hat{L}^*(w_0^-, \ldots, w_{l-1}^-) = \sum_{i=1}^{l} \frac{\xi^i}{i!} b^{(i)}(0) w_{l-i}^-.$$

Then $w^-(\xi)$ satisfies $|w^-(0)| < C, |w^-(1)| < C\mathrm{e}^{-\sqrt{b(0)/\varepsilon}}$, and

$$|(w^-)^{(p)}(x)| < C\varepsilon^{-p/2}\mathrm{e}^{-\sqrt{b(0)/\varepsilon}x}.$$

A similar argument can be used to establish the result for the right-hand boundary layer. Hence, $w(x)$ satisfies the boundary conditions and the proof is complete. □

3. Discretisation and nonuniform grids

3.1. Finite difference discretisation

We will consider difference approximations of (1) on a nonuniform partition,

$$\Delta = \{0 = x_0 < x_1 < \cdots < x_{N-1} < x_N = 1\}$$

and let $h_j = x_j - x_{j-1}$. Given the mesh function $\{\phi_j\}_{j=0}^N$, we define the following difference operator:

$$(\delta_2 \phi_\Delta)_j = \frac{2}{h_j + h_{j+1}} \left(\frac{\phi_{j+1} - \phi_j}{h_{j+1}} - \frac{\phi_j - \phi_{j-1}}{h_j} \right).$$

Then, the standard central difference discretisation of (1) takes the form

$$\begin{aligned} &(L_\Delta u_\Delta)_j = -\varepsilon(\delta_2 u_\Delta)_j + b(x_j)u_j = f(x_j), \quad 1 \leqslant j \leqslant N-1, \\ &u_0 = 0, \quad u_N = 0. \end{aligned} \tag{7}$$

3.2. Grid equidistribution

A commonly used technique in adaptive grid generation is mesh equidistribution. A grid is said to be equidistributing if

$$\int_{x_{j-1}}^{x_j} M(u(s), s)\, \mathrm{d}s = \frac{1}{N} \int_0^1 M(u(s), s)\, \mathrm{d}s, \quad j = 1, \ldots, N,$$

where $M(u(x), x) > 0$ is called a monitor function. The optimal choice of monitor function clearly depends on the problem being solved, the numerical discretisation being used, and the norm of the error to be controlled. With a view to solving singularly perturbed reaction–diffusion problems, it seems reasonable to consider numerical discretisations that are ε-uniformly stable with respect to the discrete l_∞ norm. We will see later that the central difference method falls into this category. By ignoring stability issues, the monitor function can then be tailored towards controlling the local truncation error. For most finite difference schemes the truncation error can locally be bounded by a combination of high derivatives of the exact solution: this suggests basing a monitor function on approximations of high derivatives of the unknown exact solution using the numerical solution. However, it is highly unlikely, especially in the initial stages of grid adaption, that the numerical solution will be very accurate. Hence, numerically estimating high derivatives is likely to be extremely error prone. A more pragmatic approach is to base the monitor function on a numerical approximation of a low derivative of the unknown solution. Since the main numerical difficulty in solving (1) is the presence of steep boundary layers, we consider the monitor function

$$M = \alpha + |w''(x)|^{1/m}, \tag{8}$$

where α is a positive constant that is independent of N. Equidistributing (8) with $\alpha = 0$ and $w(x)$ given by (4) results in a grid with almost all of the mesh points clustered within the boundary layers. This is due to the monitor function being practically zero external to the layers. This is unlikely to be a good mesh for numerically solving (1). To make the adaptive grid procedure more robust it is common practice to introduce a floor on the monitor function to ensure that it is bounded away

from zero and this is the role that is played by α in (8). The use of a floor ensures that some grid points are placed external to any boundary layers. Such a grid can then be expected to work well for inhomogeneous problems.

In a practical adaptive algorithm, the monitor function has to be approximated from the numerical solution and the equidistribution principle has to be discretised. For example, discretising the equidistribution principle using the midpoint rule results in the set of equations

$$M_{j+(1/2)}(x_{j+1}-x_j)=M_{j-(1/2)}(x_j-x_{j-1}),\quad j=1,2,\ldots,N-1, \tag{9}$$

where $M_{j+(1/2)}$ is an approximation to $M(u(x_{j+(1/2)}),x_{j+(1/2)})$. The coupled nonlinear set of Eqs. (7) and (9) then has to be solved simultaneously for $\{u_j,x_j\}_{j=1}^{N-1}$. Often these equations are solved in an iterative manner where system (7) is solved first using a fixed grid. This solution is then used to define a piecewise constant monitor function that can be exactly equidistributed to give a new grid. This procedure is repeated until some measure of convergence is achieved. Pryce [23] has shown that the convergence of this iterative procedure is improved by restricting the range of values of the monitor function, and in particular by ensuring that the minimum value is bounded away from zero. Often the floor is chosen in an ad hoc way and an aim of this paper is to choose it in a more satisfactory manner.

3.3. Grid structure

We now consider the structure of a grid based on equidistribution of (8) and suggest how to choose α. Taking the leading term of (5) and (6), we have the following approximation for $w''(x)$,

$$w''(x)\approx\begin{cases}-\dfrac{b(0)}{\varepsilon}v_0(0)\mathrm{e}^{-\sqrt{(b(0)/\varepsilon)}x}, & x\in[0,1/2],\\ -\dfrac{b(1)}{\varepsilon}v_0(1)\mathrm{e}^{-\sqrt{(b(1)/\varepsilon)}(1-x)}, & x\in(1/2,1].\end{cases}$$

Hence,

$$\int_0^1|w''(x)|^{1/m}\,\mathrm{d}x\equiv\Phi\approx m\varepsilon^{(m-2)/2m}\left(\frac{v(0)^{1/m}}{b(0)^{(m-2)/2m}}+\frac{v(1)^{1/m}}{b(1)^{(m-2)/2m}}\right).$$

When $x(\xi)\leqslant\frac{1}{2}$, equidistribution of (8) approximately results in the mapping

$$\frac{\alpha}{\Phi}x(\xi)+\lambda_0(1-\mathrm{e}^{-\sqrt{(b(0)/\varepsilon)}x(\xi)/m})=\xi\left(\frac{\alpha}{\Phi}+1\right), \tag{10}$$

where

$$\lambda_0=\frac{|v(0)|^{1/m}b(0)^{(2-m)/2m}}{|v(0)|^{1/m}b(0)^{(2-m)/2m}+|v(1)|^{1/m}b(1)^{(2-m)/2m}}.$$

Similarly, when $x(\xi)>1/2$, the grid points are approximately given by the relation

$$\frac{\alpha}{\Phi}(1-x(\xi))+\lambda_1(1-\mathrm{e}^{-\sqrt{(b(1)/\varepsilon)}(1-x(\xi))/m})=(1-\xi)\left(\frac{\alpha}{\Phi}+1\right),$$

where

$$\lambda_1=\frac{|v(1)|^{1/m}b(1)^{(2-m)/2m}}{|v(0)|^{1/m}b(0)^{(2-m)/2m}+|v(1)|^{1/m}b(1)^{(2-m)/2m}}.$$

A nonuniform grid $\{x_j\}_{j=0}^N$ in physical space corresponds to an equispaced grid $\{\xi_j = j/N\}_{j=0}^N$ in computational space. This identification gives the mesh

$$\frac{\alpha}{\Phi} x_j + \lambda_0(1 - \mathrm{e}^{-\sqrt{(b(0)/\varepsilon)}x_j/m}) = \frac{j}{N}\left(\frac{\alpha}{\Phi} + 1\right), \quad x_j \leqslant \frac{1}{2} \tag{11}$$

and

$$\frac{\alpha}{\Phi}(1 - x_j) + \lambda_1(1 - \mathrm{e}^{-\sqrt{(b(1)/\varepsilon)}(1-x_j)/m}) = \left(1 - \frac{j}{N}\right)\left(\frac{\alpha}{\Phi} + 1\right), \quad x_j > \frac{1}{2}. \tag{12}$$

The location of the grid point x_j is given implicitly by the solution of the nonlinear algebraic Eqs. (11) or (12). However, an important insight into the distribution of mesh points is given by the following lemma.

Lemma 3. *Assuming that the nonuniform grid* (11) *and* (12) *is generated with* $\alpha = \Phi$ *then*

$$x_{k_l} < m\sqrt{\frac{\varepsilon}{b(0)}}\log(N) < x_{k_l+1}$$

and

$$x_{k_r-1} < 1 - m\sqrt{\frac{\varepsilon}{b(1)}}\log(N) < x_{k_r},$$

where

$$k_l = \left[\frac{1}{2}\left(\lambda_0(N-1) + m\sqrt{\frac{\varepsilon}{b(0)}}N\log(N)\right)\right],$$

$$k_r = \left[N - \frac{1}{2}\left(\lambda_1(N-1) + m\sqrt{\frac{\varepsilon}{b(1)}}N\log(N)\right)\right] + 1$$

and $[\,\cdot\,]$ *denotes the integer part of.*

Proof. The value for k_l follows from substituting $x_j = m\sqrt{(\varepsilon/b(0))}\log(N)$ into (11) with $\alpha = \Phi$ and solving for j. A similar argument can be used for the right-hand layer to give k_r.

The choice of α is motivated by the analysis of difference schemes on piecewise uniform Shishkin grids: see [19]. These grids are defined as follows: let N be an integer that is exactly divisible by 4 and set

$$\tau = \min\left\{\frac{1}{4}, \tau_0\sqrt{\frac{\varepsilon}{\beta}}\log(N)\right\},$$

where $\tau_0 \geqslant 1$ is a user-chosen parameter. The domain is partitioned into three regions; $[0,\tau]$, $[\tau, 1-\tau]$, and $[1-\tau, 1]$. In each of the two boundary layer regions the grid is uniform with mesh spacing $4\tau/N$. The grid in the interior region is also uniform with mesh spacing $2(1-2\tau)/N$. By setting $\alpha = \Phi$

the equidistributed grid shares some properties of the Shishkin grid. For example, if $|v_0(0)| = |v_0(1)|$ and $b(x) = \beta$ is a constant, then $\lambda_0 = \lambda_1 = \frac{1}{2}$: if N is exactly divisible by 4 and

$$m\sqrt{\frac{\varepsilon}{\beta}}\,N\log(N) \leqslant \frac{1}{2}, \tag{13}$$

then

$$x_{(N/4)-1} < m\sqrt{\frac{\varepsilon}{\beta}}\log(N) < x_{N/4}, \quad \text{and} \quad x_{3N/4} < 1 - m\sqrt{\frac{\varepsilon}{\beta}}\log(N) < x_{(3N/4)+1}.$$

The partitioning of the equidistributed grid is clearly related to that of the Shishkin grid with m playing a similar role to τ_0. Note that condition (13) is likely to be satisfied when we adaptively solve a singularly perturbed problem.

However, the equidistributed grid differs from the Shishkin grid in three key aspects. First, the grid is exponentially stretched within the boundary layers as opposed to being uniform. The stretching is, in fact, very similar to that used in the a priori nonuniform grids of [3]. This has a beneficial effect in terms of accuracy which will be established theoretically in the next section and will be demonstrated by numerical experiments in Section 5. The second advantage of the equidistributed grid is the ability to automatically cater for different steepness of boundary layers at either end of the domain. As an extreme case, if $v_0(0) = 0$ and $v_0(1) \neq 0$, then there is only one boundary layer at $x = 1$. According to (11) and (12) the grid points automatically cluster around the one boundary layer at the right and the grid external to the layer is almost uniform. On the other hand, if the problem has two boundary layers and $|v_0(0)| \neq |v_0(1)|$, then grid equidistribution automatically determines the allocation of grid points within each layer. For example, if $m = 2$, $|v_0(0)| = 1$, and $|v_0(1)| = 4$, then $\lambda_0 = \frac{1}{3}$ and $\lambda_1 = \frac{2}{3}$. Furthermore, if we assume that N is exactly divisible by 6 and

$$m\sqrt{\frac{\varepsilon}{\beta}}\,N\log(N) < \lambda_0,$$

then

$$x_{(N/6)-1} < m\sqrt{\frac{\varepsilon}{\beta}}\,N\log(N) < x_{N/6}, \quad \text{and} \quad x_{2N/3} < 1 - m\sqrt{\frac{\varepsilon}{\beta}}\,N\log(N) < x_{(2N/3)+1}.$$

Hence, there are twice as many points within the steeper right-hand layer. In Section 5 we present numerical experiments to show that this property of the grid helps to equidistribute the error between the two boundary layers. The third advantage of the equidistributing grid is that it automatically deals with two boundary layers of different thickness, as will happen when $b(0) \neq b(1)$. This leads to a quantitative reduction in the error, since the exponential stretching of the grid does not extend beyond the edge of the boundary layers. A similar effect can be achieved for Shishkin grids by choosing

$$\tau_l = \min\left\{\frac{1}{4}, \tau_0\sqrt{\frac{\varepsilon}{b(0)}}\log(N)\right\}$$

and

$$\tau_r = 1 - \min\left\{\frac{1}{4}, \tau_0\sqrt{\frac{\varepsilon}{b(1)}}\log(N)\right\}$$

and then partitioning the domain into regions; $[0,\tau_l]$, $[\tau_l,\tau_r]$, and $[\tau_r,1]$.

Throughout the rest of this paper we will assume that $\alpha = \Phi$. We will also assume that

$$m\sqrt{\frac{\varepsilon}{b(0)}}N\log(N) < \frac{\lambda_0}{2}, \quad \text{and} \quad m\sqrt{\frac{\varepsilon}{b(1)}}N\log(N) < \frac{\lambda_1}{2}. \tag{14}$$

Note that this is not an overly restrictive assumption if $|v_0(0)|$ does not differ excessively from $|v_0(1)|$ and $N\log(N)$ is small in relation to $\sqrt{\beta/\varepsilon}$. In fact, (14) is exactly the regime for which we are interested in using an adaptive algorithm to solve (1). If either λ_0 or $\lambda_1 = 0$ then the following analysis can easily be modified to cater for only one boundary layer region. Finally, we are only interested in analysing what goes on when $N^{-1} \gg \sqrt{\varepsilon}$, otherwise a uniform grid could be used and a classical error analysis performed.

Lemma 3 suggests a partitioning of the domain: in what follows, we say that the points $\{x_j\}_{j=k_l}^{k_r}$ are outside the boundary layer regions and $\{x_j\}_{j=0}^{k_l-1}$ and $\{x_j\}_{j=k_r+1}^{N}$ are in the boundary layer regions. We now establish two useful lemmas regarding the size of the mesh widths within the boundary layer regions.

Lemma 4. *The mesh spacing inside the boundary layers satisfies*

$$h_j < Cm\sqrt{\frac{\varepsilon}{b(0)}}, \quad j = 1,2,\ldots,k_l$$

and

$$h_j < Cm\sqrt{\frac{\varepsilon}{b(1)}}, \quad j = k_r+1,\ldots,N.$$

Proof. We will only prove the result for the left-hand layer as the layer on the right can be dealt with similarly. We first establish upper and lower bounds on the location of x_j. From mapping (11), we have that $x_j < \bar{x}_j$ where

$$\mathrm{e}^{-\sqrt{(b(0)/\varepsilon)}\bar{x}_j/m} = 1 - \frac{2j}{\lambda_0 N}.$$

Therefore,

$$x_j < \bar{x}_j = -m\sqrt{\frac{\varepsilon}{b(0)}}\log\left(1 - \frac{2j}{\lambda_0 N}\right). \tag{15}$$

Using this upper bound in mapping (11) we find that

$$x_j > \underline{x}_j = -m\sqrt{\frac{\varepsilon}{b(0)}}\log\left(1 - \frac{1}{\lambda_0}\left(\frac{2j}{N} + m\sqrt{\frac{\varepsilon}{b(0)}}\log\left(1 - \frac{2j}{\lambda_0 N}\right)\right)\right). \tag{16}$$

Using (15) and (16) we have for $j = 1, 2, \ldots, k_l$ that

$$h_j < \bar{x}_j - \underline{x}_{j-1} = m\sqrt{\frac{\varepsilon}{b(0)}}\log\left(1 + \frac{2 + m\sqrt{(\varepsilon/b(0))}N\log(\lambda_0 N/(\lambda_0 N - 2(j-1)))}{\lambda_0 N - 2j}\right)$$
$$< Cm\sqrt{\frac{\varepsilon}{b(0)}}.$$

Lemma 5. *Inside the two boundary layer regions*

$$|h_{j+1} - h_j| \leqslant \begin{cases} Ch_j^2, & j = 1, \ldots, k_l - 1, \\ Ch_{j+1}^2, & j = k_r + 1, \ldots, N - 1. \end{cases}$$

Proof. First, we look at the left-hand boundary. In terms of computational coordinates

$$\frac{|h_{j+1} - h_j|}{h_j^2} \leqslant \frac{2|x_{\xi\xi}(\eta_j^{(1)})|}{(x_\xi(\eta_j^{(2)}))^2},$$

where $\eta_j^{(1)} \in (\xi_{j-1}, \xi_{j+1})$ and $\eta_j^{(2)} \in (\xi_{j-1}, \xi_j)$. From (10) with $\alpha = \Phi$, we have

$$x_\xi(\eta) = \frac{2m\sqrt{\varepsilon/b(0)}}{(m\sqrt{\varepsilon/b(0)} + \lambda_0 e^{-\sqrt{(b(0)/\varepsilon)}x(\eta)/m})} \quad \text{and} \quad x_{\xi\xi}(\eta) = \frac{4m\lambda_0\sqrt{(\varepsilon/b(0))}e^{-\sqrt{(b(0)/\varepsilon)}x(\eta)/m}}{(m\sqrt{(\varepsilon/b(0))} + \lambda_0 e^{-\sqrt{(b(0)/\varepsilon)}x(\eta)/m})^3}.$$

Therefore,

$$\frac{|h_{j+1} - h_j|}{h_j^2} \leqslant \frac{\lambda_0\sqrt{b(0)/\varepsilon}(\lambda_0 e^{-\sqrt{(b(0)/\varepsilon)}x_{j-1}/m} + m\sqrt{b(0)/\varepsilon})^2}{m(\lambda_0 e^{-\sqrt{(b(0)/\varepsilon)}x_{j+1}/m} + m\sqrt{b(0)/\varepsilon})^3} \leqslant C.$$

The bound on the mesh spacings at the right-hand boundary is obtained in a similar manner.

This lemma shows that the equidistributed grid is uniformly locally quasi-uniform within the two boundary layer regions. However, the ratio of the grid cells between the boundary layer and outside the boundary layer regions is proportional to $\varepsilon^{-1/2}$. Hence, the grid is not uniformly locally quasi-uniform across the whole domain and this is reflected in the analysis that follows in the next section.

4. Error analysis

As for the exact solution, we decompose the numerical solution such that

$$u_j = W_j + V_j, \quad j = 0, \ldots, N,$$

where

$$(L_\Delta W_\Delta)_j = 0, \quad W_0 = w(0), \quad W_N = w(1)$$

and

$$(L_\Delta V_\Delta)_j = f_j, \quad V_0 = v(0), \quad V_N = v(1).$$

The error may be expressed as

$$|u(x_j) - u_j| \leqslant |w(x_j) - W_j| + |v(x_j) - V_j|.$$

Hence, we have only to bound the errors in the smooth and singular components of the numerical solution, separately.

To derive the error estimates we first state a number of lemmas that are essential to the analysis.

Lemma 6 (The discrete maximum principle). *The system* $(L_\Delta u_\Delta)_j = f_j$, *with* u_0 *and* u_N *specified, has a unique solution. If* $(L_\Delta u_\Delta)_j < (L_\Delta v_\Delta)_j$, $1 \leqslant j \leqslant N-1$, *and if* $u_0 < v_0$, $u_N < v_N$, *then* $u_j < v_j$, $1 \leqslant j \leqslant N-1$.

Proof. It is easy to verify that the matrix associated with L_Δ is an irreducible M-matrix, and so has a positive inverse. Hence, the result follows.

Lemma 7. *Let* $(z_\Delta)_j = 1 + x_j$ *for* $0 \leqslant j \leqslant N$. *Then there exists a positive constant* C *such that* $(L_\Delta z_\Delta)_j \geqslant C$ *for* $1 \leqslant j \leqslant N-1$.

Proof. This is an easy computation.

From Lemma 7 it follows that $\|L_\Delta^{-1}\|_\infty$ is uniformly bounded independently of N and ε. To uniformly bound the error in the solution we therefore have only to derive an ε-independent bound on the local truncation error.

4.1. The error in the singular component

To bound the truncation error in the singular component of the solution we separately consider the regions of the domain inside and outside the boundary layers.

Lemma 8. *For* $j = k_l, \ldots, k_r$

$$|\tau_j^W| \leqslant CN^{-m}.$$

Proof. The truncation error satisfies

$$\tau_j^W = (L_\Delta(R_\Delta w))_j - (Lw)(x_j),$$

where R_Δ is a restriction operator such that $(R_\Delta w)_j = w(x_j)$. Therefore,

$$|\tau_j^W| = \varepsilon |(\delta_2 R_\Delta w)_j - w''(x_j)|.$$

Using two applications of the mean value theorem, it is easy to show that

$$|(\delta_2 R_\Delta w)_j| \leqslant 2 \max_{x_{j-1} \leqslant x \leqslant x_{j+1}} |w''(x)|.$$

Hence,

$$|\tau_j^W| \leqslant 3\varepsilon \max_{x_{j-1} \leqslant x \leqslant x_{j+1}} |w''(x)|.$$

Therefore,

$$|\tau_j^W| \leqslant C \begin{cases} \mathrm{e}^{-\sqrt{(b(0)/\varepsilon)}x_{j-1}}, & x_j \leqslant \frac{1}{2}, \\ \mathrm{e}^{-\sqrt{(b(1)/\varepsilon)}(1-x_{j+1})}, & x_j > \frac{1}{2}. \end{cases}$$

When $k_l \leqslant j$ and $x_j \leqslant \frac{1}{2}$

$$|\tau_j^W| \leqslant C\mathrm{e}^{-\sqrt{(b(0)/\varepsilon)}x_{k_l-1}} = C(\mathrm{e}^{-\sqrt{(b(0)/\varepsilon)}x_{k_l-1}/m})^m.$$

From the grid equidistribution condition (11), we have

$$\begin{aligned} \mathrm{e}^{-\sqrt{(b(0)/\varepsilon)}x_{k_l-1/m}} &= \frac{1}{\lambda_0}\left(x_{k_l-1} + \lambda_0 - \frac{2(k_l-1)}{N}\right) \\ &\leqslant \frac{1}{\lambda_0}\left(m\sqrt{\frac{\varepsilon}{b(0)}}\log(N) + \lambda_0 - \frac{1}{N}\left(\lambda_0(N-1) + m\sqrt{\frac{\varepsilon}{b(0)}}N\log(N) - 4\right)\right) \\ &\leqslant CN^{-1}. \end{aligned}$$

Therefore, for $k_l \leqslant j$ and $x_j \leqslant \frac{1}{2}$

$$|\tau_j^W| \leqslant CN^{-m}.$$

A similar argument establishes the same bound for $j \leqslant k_r$ and $x_j > \frac{1}{2}$.

The truncation error in the boundary layer regions is treated in a different manner.

Lemma 9. *For $j = 1, \ldots, k_l - 1$ and $j = k_r + 1, \ldots, N-1$,*

$$|\tau_j^W| \leqslant C \begin{cases} N^{-2}, & m \geqslant 2, \\ N^{-m}, & m < 2. \end{cases}$$

Proof. We will only give details of the boundary region on the left as the right-hand boundary region can be dealt with analogously. Using Taylor expansions it can be shown that

$$|\tau_j^W| = \frac{\varepsilon|h_{j+1}^2 w'''(\eta_j^{(1)}) - h_j^2 w'''(\eta_j^{(2)})|}{3(h_{j+1}+h_j)},$$

where $\eta_j^{(1)} \in (x_j, x_{j+1})$ and $\eta_j^{(2)} \in (x_{j-1}, x_j)$. Furthermore,

$$\begin{aligned} |h_{j+1}^2 w'''(\eta_j^{(1)}) - h_j^2 w'''(\eta_j^{(2)})| &\leqslant |h_{j+1}^2 - h_j^2||w'''(\eta_j^{(1)})| + h_j^2|w'''(\eta_j^{(1)}) - w'''(\eta_j^{(2)})| \\ &\leqslant C(|h_{j+1}^2 - h_j^2||w'''(x_j)| + h_j^2(h_{j+1}+h_j)|w^{(iv)}(x_j)|), \end{aligned}$$

which follows using Lemma 4 and the fact that $|\eta_j^{(1)} - \eta_j^{(2)}| < (h_{j+1} + h_j)$. Therefore, we have

$$\begin{aligned} |\tau_j^W| &\leqslant C\sqrt{\varepsilon}h_j^2|w'''(x_j)| \\ &\leqslant C\varepsilon^{-1}h_j^2\mathrm{e}^{-\sqrt{(b(0)/\varepsilon)}x_j}. \end{aligned}$$

The rest of the proof depends on the value of m. If $m \geqslant 2$ then

$$|\tau_j^W| \leqslant C\varepsilon^{-1}\left(\int_{x_{j-1}}^{x_j} \mathrm{e}^{-\sqrt{(b(0)/\varepsilon)}s/m}\,\mathrm{d}s\right)^2 \leqslant C\varepsilon^{-1}\left(\varepsilon^{1/m}\int_{x_{j-1}}^{x_j} M(u(s),s)\,\mathrm{d}s\right)^2$$
$$\leqslant C\varepsilon^{(2-m)/m}\Phi^2 N^{-2} \leqslant CN^{-2}.$$

On the other hand, if $m < 2$ then

$$|\tau_j^W| \leqslant C\varepsilon^{-1}h_j^{2-m}(h_j\mathrm{e}^{-\sqrt{(b(0)/\varepsilon)}x_j/m})^m \leqslant C\varepsilon^{(2-m)/2}\left(\int_{x_{j-1}}^{x_j} M(u(s),s)\,\mathrm{d}s\right)^m$$
$$\leqslant C\varepsilon^{(2-m)/2}\Phi^m N^{-m} \leqslant CN^{-m}.$$

Note the extremely convenient role that the equidistribution principle plays in the proof above. A similar technique is used in the analysis of [1,22].

4.2. The error in the smooth component

Lemma 10. *For* $j = 1,\ldots,N-1$

$$|\tau_j^V| \leqslant CN^{-2}.$$

Proof. Using Taylor series expansions it is easy to show that

$$|\tau_j^V| \leqslant C\varepsilon(h_{j+1}+h_j)\max_{x_{j-1}\leqslant x\leqslant x_{j+1}}|v'''(x)|.$$

It is also easy to deduce from grids (11) and (12) that

$$(h_j + h_{j+1}) \leqslant CN^{-1} \quad \text{for } j = 1,\ldots,N-1.$$

The result then follows from bound (3) and the assumption that $N^{-1} \gg \sqrt{\varepsilon}$.

We now state the main theorems of this paper.

Theorem 11. *Let* $u(x)$ *be the exact solution of* (1) *and let* u_Δ *be obtained from* (7) *on the grids defined by* (11) *and* (12) *with* $\alpha = \Phi$. *Assuming the conditions* (14) *hold then there exists a constant* C, *independent of* N *and* ε, *such that for* $j = 1,\ldots,N-1$

$$|u(x_j) - u_j| \leqslant C\begin{cases} N^{-2}, & m \geqslant 2,\\ N^{-m}, & m < 2.\end{cases}$$

Proof. The proof is an immediate consequence of Lemmas 8–10, and the ε-uniform boundedness of $\|L_\Delta^{-1}\|_\infty$.

The uniform convergence rate on the equidistributed grid is superior to that predicted on a Shishkin grid. It has been shown in [19] that the error using the standard central difference scheme on a Shishkin mesh with $\tau_0 = 1$ converges uniformly at the rate of $\mathrm{O}(N^{-1}\log(N))$. If $\tau_0 \geqslant 2$, the analysis in [19] can easily be modified to predict the improved rate of convergence of $\mathrm{O}(N^{-2}\log(N)^2)$.

This sub-second-order rate of convergence is due to the uniform grid spacing within the boundary layer. The exponential stretching of the equidistributed grid therefore leads theoretically to improved accuracy. This will be confirmed in the next section.

The analysis above shows that the central difference scheme on the equidistributed grid is uniformly accurate at all of the grid nodes. We can construct a global approximation by forming the piecewise linear interpolant of the numerical solution. We now show that this global approximation is uniformly accurate at all points in the domain.

Theorem 12. *Let $\overline{u}(x)$ denote the piecewise linear interpolant of the central difference solution obtained as described in Theorem* 11. *Then $\overline{u}(x)$ satisfies the ε-uniform estimate*

$$\max_{x\in[0,1]} |u(x)-\overline{u}(x)| \leqslant C \begin{cases} N^{-2}, & m \geqslant 2, \\ N^{-m}, & m < 2. \end{cases}$$

Proof. For $x \in (x_{j-1}, x_j)$

$$\overline{u}(x) = u_{j-1}\varphi_{j-1}(x) + u_j\varphi_j(x),$$

where φ_{j-1}, φ_j are the Lagrange polynomials of first degree

$$\varphi_{j-1}(x) = \frac{x_j - x}{x_j - x_{j-1}}, \quad \varphi_j(x) = \frac{x - x_{j-1}}{x_j - x_{j-1}}.$$

We also define the piecewise linear interpolant of the data $\{x_j, u(x_j)\}_{j=0}^N$ by

$$\tilde{u}(x) = u(x_{j-1})\varphi_{j-1}(x) + u(x_j)\varphi_j(x).$$

When $x \in (x_{j-1}, x_j)$, the error

$$|u(x)-\overline{u}(x)| \leqslant |u(x)-\tilde{u}(x)| + |\tilde{u}(x)-\overline{u}(x)|.$$

Using Theorem 11 we can easily bound the second term since

$$\begin{aligned} |\tilde{u}(x)-\overline{u}(x)| &\leqslant |(u(x_{j-1})-u_{j-1})\varphi_{j-1}(x)| + |(u(x_j)-u_j)\varphi_j(x)| \\ &\leqslant C \begin{cases} N^{-2}, & m \geqslant 2, \\ N^{-m}, & m < 2. \end{cases} \end{aligned}$$

All that remains is to bound the interpolation error. Using the decomposition of the exact and the numerical solutions, we have

$$|u(x)-\tilde{u}(x)| \leqslant |w(x)-\tilde{w}(x)| + |v(x)-\tilde{v}(x)|.$$

From standard interpolation theory

$$\max_{x\in(x_{j-1},x_j)} |w(x)-\tilde{w}(x)| \leqslant Ch_j^2 |w''(\eta_j)|,$$

where $\eta_j \in [x_{j-1}, x_j]$. For $j \leqslant k_l - 1$ we have from Lemma 4 that

$$|w''(\eta_j)| \leqslant C\varepsilon^{-1} \mathrm{e}^{-\sqrt{(b(0)/\varepsilon)}x_j} \mathrm{e}^{\sqrt{(b(0)/\varepsilon)}h_j} \leqslant C\varepsilon^{-1} \mathrm{e}^{-\sqrt{(b(0)/\varepsilon)}x_j}.$$

Therefore,

$$\max_{x\in(x_{j-1},x_j)} |w(x)-\tilde{w}(x)| \leqslant C\varepsilon^{-1} h_j^2 \mathrm{e}^{-\sqrt{(b(0)/\varepsilon)}x_j}, \quad j \leqslant k_l - 1.$$

Following the identical steps to those at the end of Lemma 9, we have that

$$\max_{x\in(x_{j-1},x_j)} |w(x)-\tilde{w}(x)| \leqslant C \begin{cases} N^{-2}, & m \geqslant 2, \\ N^{-m}, & m < 2, \end{cases} \qquad j \leqslant k_l - 1.$$

A similar argument establishes the same result for $j \geqslant k_r + 1$. Outside the boundary layer regions, when $j \geqslant k_l$ and $x_j \leqslant \frac{1}{2}$, we have

$$\begin{aligned} \max_{x\in(x_{j-1},x_j)} |w(x)-\tilde{w}(x)| &\leqslant \max_{x\in(x_{j-1},x_j)} (|w(x)| + |\tilde{w}(x)|) \\ &\leqslant C\mathrm{e}^{-\sqrt{(b(0)/\varepsilon)}x_{k_l-1}} = C(\mathrm{e}^{-\sqrt{(b(0)/\varepsilon)}x_{k_l-1}/m})^m. \end{aligned}$$

Following the same argument as in Lemma 8, we have

$$\max_{x\in(x_{j-1},x_j)} |w(x)-\tilde{w}(x)| \leqslant CN^{-m}.$$

A similar procedure is used when $j \leqslant k_r$ and $x_j > \frac{1}{2}$.

For the interpolant of the smooth component we have

$$|v(x)-\tilde{v}(x)| \leqslant Ch_j^2 |v''(\eta_j)|,$$

where $x_{j-1} \leqslant \eta_j \leqslant x_j$. Using the bound (3) we have

$$|v(x)-\tilde{v}(x)| \leqslant CN^{-2}.$$

This completes the proof. □

The above analysis clearly indicates the advantage of taking $m \geqslant 2$ if the overall aim is to control the error in the L_∞-norm. Another norm that is often of interest for reaction–diffusion problems is the energy-norm defined by

$$\|u\|_E^2 \equiv \varepsilon \|u'\|_{L_2}^2 + \|b(x)^{1/2}u\|_{L_2}^2.$$

For the Galerkin finite element method using piecewise linear basis functions, it has been shown that the error minimising grid equidistributes an a posteriori error estimate that is asymptotically equivalent to the function $M = |u''|^{2/3}$ (see [2,26]). The same monitor is related to the characterisation of optimal grids based on piecewise linear interpolation (see [8]). There is clearly a connection to our monitor function with $m = \frac{3}{2}$.

5. Numerical experiments

Example 1. The problem

$$-\varepsilon u''(x) + u(x) = x, \quad u(0) = u(1) = 0$$

has an analytic solution with a boundary layer at $x = 1$ and is essentially linear external to the layer. Table 1 shows the maximum nodal error and the L_2 error for two representative values of ε where the grid has been obtained by equidistributing $w(x)$. We clearly observe uniform second-order convergence. To vindicate the analysis pursued in this paper, we also consider a truly adaptive

Table 1
Central difference results for Example 1 using exact equidistribution with $m = 3$

N	$\varepsilon = 1 \cdot 10^{-8}$				$\varepsilon = 1 \cdot 10^{-16}$			
	$\|e\|_\infty$	Rate	$\|e\|_{L_2}$	Rate	$\|e\|_\infty$	Rate	$\|e\|_{L_2}$	Rate
32	$4.245 \cdot 10^{-4}$	—	$3.344 \cdot 10^{-5}$	—	$4.261 \cdot 10^{-4}$	—	$3.341 \cdot 10^{-7}$	—
64	$1.055 \cdot 10^{-4}$	2.01	$8.368 \cdot 10^{-6}$	2.00	$1.058 \cdot 10^{-4}$	2.01	$8.370 \cdot 10^{-8}$	2.00
128	$2.635 \cdot 10^{-5}$	2.00	$2.093 \cdot 10^{-6}$	2.00	$2.644 \cdot 10^{-5}$	2.00	$2.094 \cdot 10^{-8}$	2.00
256	$6.586 \cdot 10^{-6}$	2.00	$5.232 \cdot 10^{-7}$	2.00	$6.608 \cdot 10^{-6}$	2.00	$5.235 \cdot 10^{-9}$	2.00
512	$1.646 \cdot 10^{-6}$	2.00	$1.308 \cdot 10^{-7}$	2.00	$1.652 \cdot 10^{-6}$	2.00	$1.309 \cdot 10^{-9}$	2.00

Table 2
Central difference results for Example 1 using approximate equidistribution with $m = 3$

N	$\varepsilon = 1 \cdot 10^{-8}$				$\varepsilon = 1 \cdot 10^{-16}$			
	$\|e\|_\infty$	Rate	$\|e\|_{L_2}$	Rate	$\|e\|_\infty$	Rate	$\|e\|_{L_2}$	Rate
32	$5.391 \cdot 10^{-4}$	—	$4.526 \cdot 10^{-5}$	—	$6.666 \cdot 10^{-4}$	—	$5.702 \cdot 10^{-7}$	—
64	$1.191 \cdot 10^{-4}$	2.18	$9.564 \cdot 10^{-6}$	2.40	$1.342 \cdot 10^{-4}$	2.31	$1.075 \cdot 10^{-7}$	2.14
128	$2.790 \cdot 10^{-5}$	2.09	$2.222 \cdot 10^{-6}$	2.18	$2.986 \cdot 10^{-5}$	2.17	$2.371 \cdot 10^{-8}$	2.03
256	$6.761 \cdot 10^{-6}$	2.04	$5.375 \cdot 10^{-7}$	2.07	$7.111 \cdot 10^{-6}$	2.07	$5.637 \cdot 10^{-9}$	1.98
512	$1.667 \cdot 10^{-6}$	2.02	$1.325 \cdot 10^{-7}$	2.02	$1.751 \cdot 10^{-6}$	2.02	$1.388 \cdot 10^{-9}$	2.02

solution of (1), where we simultaneously solve (7) and (9). To calculate $M_{j+(1/2)}$, we require an approximation of $w''(x_{j+(1/2)})$. At the interior nodes we set

$$w''(x_j) \approx \tilde{w}''_j \equiv \left(\delta_2\left(u_\Delta - R_\Delta\left(\frac{f}{b}\right)\right)\right)_j, \quad j = 1, \ldots, N-1.$$

At x_0 and x_N we use an optimal four point formula using the fast algorithm of Fornberg [13]. Finally, the monitor function is defined by

$$M_{j+(1/2)} = \left(\sum_{k=0}^{N-1} h_{k+1}\left|\frac{\tilde{w}''_k + \tilde{w}''_{k+1}}{2}\right|^{1/m}\right) + \left|\frac{\tilde{w}''_j + \tilde{w}''_{j+1}}{2}\right|^{1/m}, \quad j = 0, \ldots, N-1.$$

From Table 2, we see that we again have uniform second-order convergence and the errors are very similar to those obtained using exact equidistribution of the analytic solution. For comparison, Table 3 shows the results obtained using a Shishkin grid where we have attempted to use an optimal value of the parameter τ_0. The table clearly indicates that the nodal errors are uniformly convergent at the rate of $O(N^{-2}\log(N)^2)$. This sub-second-order convergence rate results in the errors being considerably larger than those obtained using the equidistributed grid. Hence, a significant gain in accuracy can be obtained from the exponential stretching of the grid within the boundary layer.

To investigate the dependence of the errors on the choice of m, Fig. 1 shows the results when $\varepsilon = 1 \cdot 10^{-16}$. It is clear from this plot that something special happens when $m = 4$. In the appendix it is shown that the truncation error of the singular component of the solution is fourth order when $m = 4$.

Table 3
Central difference results for Example 1 using a Shishkin grid with $\tau_0 = 2$

N	$\varepsilon = 1 \cdot 10^{-8}$				$\varepsilon = 1 \cdot 10^{-16}$			
	$\|e\|_\infty$	Rate	$\|e\|_{L_2}$	Rate	$\|e\|_\infty$	Rate	$\|e\|_{L_2}$	Rate
32	$2.797 \cdot 10^{-3}$	—	$1.469 \cdot 10^{-4}$	—	$2.797 \cdot 10^{-3}$	—	$1.469 \cdot 10^{-6}$	—
64	$1.028 \cdot 10^{-3}$	1.44	$5.348 \cdot 10^{-5}$	1.46	$1.028 \cdot 10^{-3}$	1.44	$5.348 \cdot 10^{-7}$	1.46
128	$3.510 \cdot 10^{-4}$	1.55	$1.827 \cdot 10^{-5}$	1.55	$3.510 \cdot 10^{-4}$	1.55	$1.827 \cdot 10^{-7}$	1.55
256	$1.149 \cdot 10^{-4}$	1.61	$5.973 \cdot 10^{-6}$	1.61	$1.149 \cdot 10^{-4}$	1.61	$5.973 \cdot 10^{-8}$	1.61
512	$3.639 \cdot 10^{-5}$	1.66	$1.891 \cdot 10^{-6}$	1.66	$3.639 \cdot 10^{-5}$	1.66	$1.891 \cdot 10^{-8}$	1.66

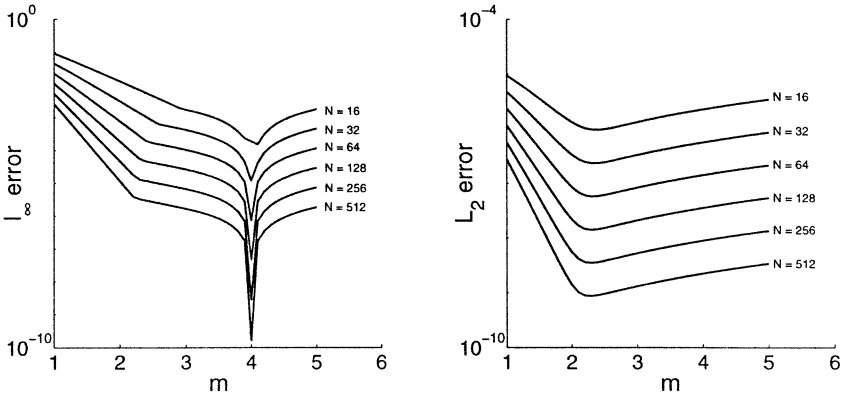

Fig. 1. Error variation with m for Example 1 with $\varepsilon = 1 \cdot 10^{-16}$ using equidistributed grids.

However, the truncation error of the smooth component is still second order when $m = 4$. We could therefore expect that the total error will be fourth order in cases where the error is dominated by that of the singular component. This improvement in accuracy from second to fourth order is closely related to other choices of special nonuniform grids [6,7,9]. Fig. 2 shows the results obtained by varying τ_0 in the definition of a Shishkin grid and we can see that the errors are relatively insensitive when $\tau_0 > \frac{3}{2}$.

Example 2. A problem with boundary layers of different heights is

$$-\varepsilon u''(x) + u(x) = 1 - 3x\cos(\pi x), \quad u(0) = u(1) = 0.$$

For this example the equidistributed grid automatically allocates more points within the steeper right-hand boundary layer. The results using the equidistributed grids are shown in Tables 4 and 5 and we can see that the errors converge at the rate expected. The results using a Shishkin grid in Table 6 are much poorer than those using the equidistributed grid. By design, the Shishkin grid pays no attention to the relative size of the two boundary layers and thus the error in one layer is considerably larger than in the other. Mesh equidistribution, as the name suggests, attempts to disperse the error equally throughout the grid. Fig. 3 show the results obtained for a typical case.

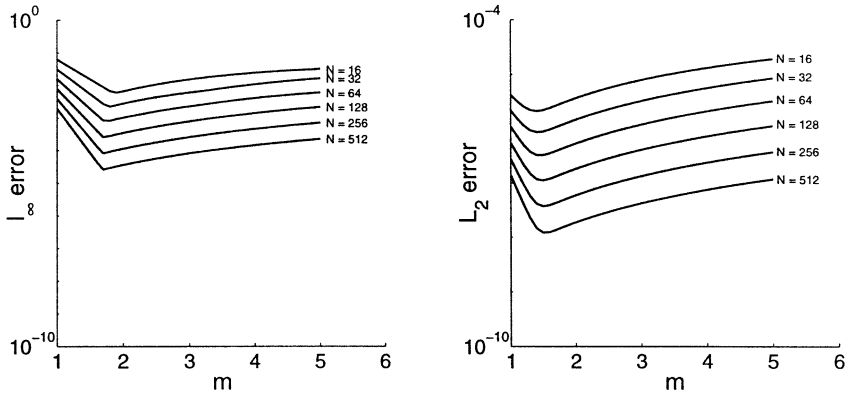

Fig. 2. Error variation with τ_0 for Example 1 with $\varepsilon = 1 \cdot 10^{-16}$ using Shishkin grids.

Table 4
Central difference results for Example 2 using exact equidistribution with $m = 3$

N	$\varepsilon = 1 \cdot 10^{-8}$				$\varepsilon = 1 \cdot 10^{-16}$			
	$\|e\|_\infty$	Rate	$\|e\|_{L_2}$	Rate	$\|e\|_\infty$	Rate	$\|e\|_{L_2}$	Rate
32	$4.559 \cdot 10^{-3}$	—	$5.607 \cdot 10^{-3}$	—	$4.585 \cdot 10^{-3}$	—	$5.591 \cdot 10^{-3}$	—
64	$1.122 \cdot 10^{-3}$	2.02	$1.406 \cdot 10^{-3}$	2.00	$1.128 \cdot 10^{-3}$	2.02	$1.402 \cdot 10^{-3}$	2.00
128	$2.793 \cdot 10^{-4}$	2.01	$3.527 \cdot 10^{-4}$	2.00	$2.811 \cdot 10^{-4}$	2.00	$3.525 \cdot 10^{-4}$	1.99
256	$6.962 \cdot 10^{-5}$	2.00	$8.918 \cdot 10^{-5}$	1.98	$7.024 \cdot 10^{-5}$	2.00	$8.882 \cdot 10^{-5}$	1.99
512	$1.722 \cdot 10^{-5}$	2.02	$2.241 \cdot 10^{-5}$	1.99	$1.755 \cdot 10^{-5}$	2.00	$2.231 \cdot 10^{-5}$	1.99

Table 5
Central difference results for Example 2 using approximate equidistribution with $m = 3$

N	$\varepsilon = 1 \cdot 10^{-8}$				$\varepsilon = 1 \cdot 10^{-16}$			
	$\|e\|_\infty$	Rate	$\|e\|_{L_2}$	Rate	$\|e\|_\infty$	Rate	$\|e\|_{L_2}$	Rate
32	$6.961 \cdot 10^{-3}$	—	$5.159 \cdot 10^{-3}$	—	$8.514 \cdot 10^{-3}$	—	$5.644 \cdot 10^{-3}$	—
64	$1.516 \cdot 10^{-3}$	2.20	$1.308 \cdot 10^{-3}$	1.98	$1.778 \cdot 10^{-3}$	2.26	$1.409 \cdot 10^{-3}$	2.00
128	$3.343 \cdot 10^{-4}$	2.18	$3.284 \cdot 10^{-4}$	1.99	$3.507 \cdot 10^{-4}$	2.34	$3.502 \cdot 10^{-4}$	2.01
256	$7.840 \cdot 10^{-5}$	2.09	$8.248 \cdot 10^{-5}$	1.99	$7.894 \cdot 10^{-5}$	2.15	$8.779 \cdot 10^{-5}$	2.00
512	$1.888 \cdot 10^{-5}$	2.05	$2.079 \cdot 10^{-5}$	1.99	$1.885 \cdot 10^{-5}$	2.07	$2.189 \cdot 10^{-5}$	2.00

The vertical lines on the solution plots show the location of the points $x = m\sqrt{(\varepsilon/b(0))}\log(N)$ and $x = 1 - m\sqrt{(\varepsilon/b(1))}\log(N)$. We can see that there are approximately twice as many points within the steeper right-hand layer than in the layer at the left and that the error is evenly distributed between the two boundary layers. Fig. 4 shows the results obtained using a Shishkin grid where the vertical

Table 6
Central difference results for Example 2 using a Shishkin grid with $\tau_0 = 2$

N	$\varepsilon = 1 \cdot 10^{-8}$				$\varepsilon = 1 \cdot 10^{-16}$			
	$\|e\|_\infty$	Rate	$\|e\|_{L_2}$	Rate	$\|e\|_\infty$	Rate	$\|e\|_{L_2}$	Rate
32	$4.263 \cdot 10^{-2}$	—	$6.134 \cdot 10^{-3}$	—	$4.263 \cdot 10^{-2}$	—	$5.702 \cdot 10^{-3}$	—
64	$1.617 \cdot 10^{-2}$	1.40	$1.665 \cdot 10^{-3}$	1.88	$1.616 \cdot 10^{-2}$	1.40	$1.429 \cdot 10^{-3}$	2.00
128	$5.567 \cdot 10^{-3}$	1.54	$4.648 \cdot 10^{-4}$	1.84	$5.566 \cdot 10^{-3}$	1.54	$3.573 \cdot 10^{-4}$	2.00
256	$1.840 \cdot 10^{-3}$	1.60	$1.326 \cdot 10^{-4}$	1.81	$1.835 \cdot 10^{-3}$	1.60	$8.935 \cdot 10^{-5}$	2.00
512	$5.820 \cdot 10^{-4}$	1.66	$3.834 \cdot 10^{-5}$	1.79	$5.819 \cdot 10^{-4}$	1.66	$2.234 \cdot 10^{-5}$	2.00

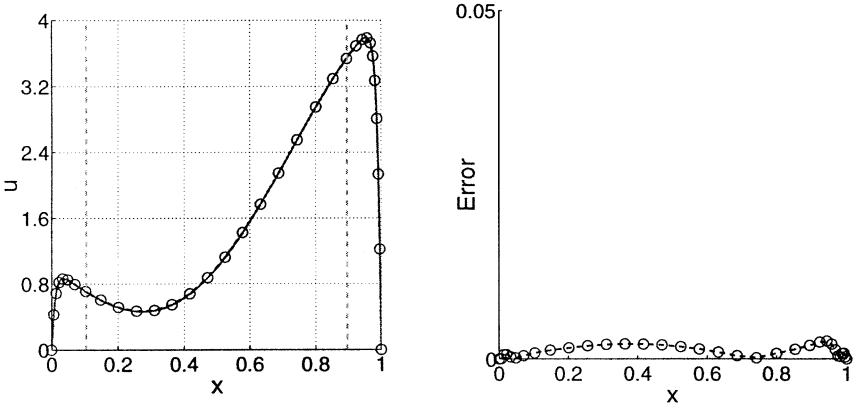

Fig. 3. Numerical solution and error using approximate equidistribution for Example 2 with $m = 3$, $N = 32$, and $\varepsilon = 1 \cdot 10^{-2}$.

lines denote the points $x = \tau_0\sqrt{(\varepsilon/\beta)}\log(N)$ and $x = 1 - \tau_0\sqrt{(\varepsilon/\beta)}\log(N)$. We can clearly see that the error in the steeper right-hand layer is considerably larger using the Shishkin grid.

Example 3. For the final example, we consider the nonconstant coefficient problem

$$-\varepsilon u''(x) + (1+x)^2 u(x) = (12x^2 - 13x + 5)(1+x)^2, \quad u(0) = u(1) = 0.$$

Note that the boundary layer on the left for this example is approximately twice as thick as the layer on the right. Results using an exactly equidistributing grid, a truly adaptive grid and a Shishkin grid are shown in Tables 7, 8 and 9, respectively: as no exact solution to this problem is available, the discrete approximations are compared with a high-order numerical solution on the exactly equidistributed grid with $N = 1024$. Again we see second-order uniform convergence with the equidistributed grids and sub-second-order convergence using the Shishkin grid. Figs. 5 and 6 show the solution and errors on the truly adapted grid and the Shishkin grid. The vertical lines on the equidistributed plot denote the location of the points $x = m\sqrt{(\varepsilon/b(0))}\log(N)$ and $x = 1 - m\sqrt{(\varepsilon/b(1))}\log(N)$. On the Shishkin plot the vertical lines denote the points $x = \tau_0\sqrt{(\varepsilon/\beta)}\log(N)$ and $x = 1 - \tau_0\sqrt{(\varepsilon/\beta)}\log(N)$. Again, we see a more balanced error distribution using the equidistributed grid as opposed to the asymmetric error distribution using the Shishkin grid.

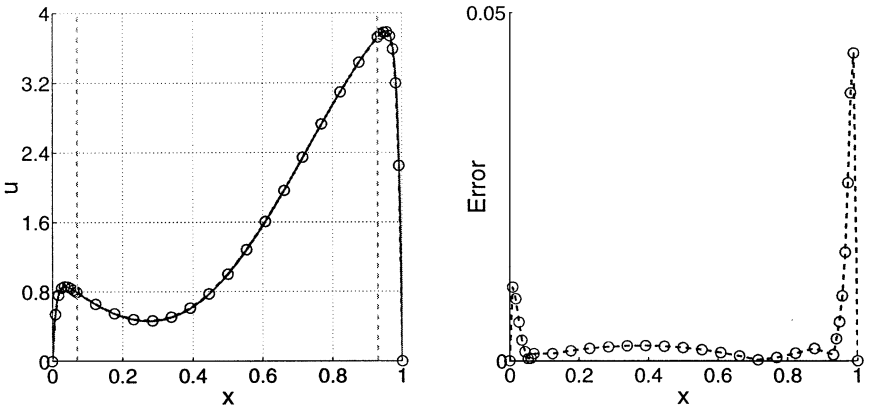

Fig. 4. Numerical solution and error using a Shishkin grid for Example 2 with $\tau_0 = 2$, $N = 32$, and $\varepsilon = 1 \cdot 10^{-2}$.

Table 7
Central difference results for Example 3 using exact equidistribution with $m = 3$

N	$\varepsilon = 1 \cdot 10^{-8}$				$\varepsilon = 1 \cdot 10^{-16}$			
	$\|e\|_\infty$	Rate	$\|e\|_{L_2}$	Rate	$\|e\|_\infty$	Rate	$\|e\|_{L_2}$	Rate
32	$8.523 \cdot 10^{-3}$	—	$8.381 \cdot 10^{-3}$	—	$8.575 \cdot 10^{-3}$	—	$8.355 \cdot 10^{-3}$	—
64	$2.070 \cdot 10^{-3}$	2.04	$2.114 \cdot 10^{-3}$	1.98	$2.082 \cdot 10^{-3}$	2.04	$2.108 \cdot 10^{-3}$	1.99
128	$5.137 \cdot 10^{-4}$	2.01	$5.335 \cdot 10^{-4}$	1.99	$5.170 \cdot 10^{-4}$	2.01	$5.343 \cdot 10^{-4}$	1.98
256	$1.306 \cdot 10^{-4}$	1.98	$1.332 \cdot 10^{-4}$	2.00	$1.290 \cdot 10^{-4}$	2.00	$1.336 \cdot 10^{-4}$	2.00
512	$3.370 \cdot 10^{-5}$	1.96	$3.315 \cdot 10^{-5}$	2.01	$3.225 \cdot 10^{-5}$	2.00	$3.340 \cdot 10^{-5}$	2.00

Table 8
Central difference results for Example 3 using approximate equidistribution with $m = 3$

N	$\varepsilon = 1 \cdot 10^{-8}$				$\varepsilon = 1 \cdot 10^{-16}$			
	$\|e\|_\infty$	Rate	$\|e\|_{L_2}$	Rate	$\|e\|_\infty$	Rate	$\|e\|_{L_2}$	Rate
32	$9.374 \cdot 10^{-3}$	—	$8.224 \cdot 10^{-3}$	—	$1.131 \cdot 10^{-2}$	—	$8.380 \cdot 10^{-3}$	—
64	$2.981 \cdot 10^{-3}$	1.65	$2.058 \cdot 10^{-3}$	2.00	$3.583 \cdot 10^{-3}$	1.66	$2.109 \cdot 10^{-3}$	1.99
128	$6.741 \cdot 10^{-4}$	2.14	$5.153 \cdot 10^{-4}$	2.00	$7.349 \cdot 10^{-4}$	2.29	$5.279 \cdot 10^{-4}$	2.00
256	$1.595 \cdot 10^{-4}$	2.08	$1.291 \cdot 10^{-4}$	2.00	$1.655 \cdot 10^{-4}$	2.15	$1.318 \cdot 10^{-4}$	2.00
512	$3.905 \cdot 10^{-5}$	2.03	$3.228 \cdot 10^{-5}$	2.00	$3.940 \cdot 10^{-5}$	2.07	$3.276 \cdot 10^{-5}$	2.01

Table 9
Central difference results for Example 3 using a Shishkin grid with $\tau_0 = 2$

N	$\varepsilon = 1 \cdot 10^{-8}$				$\varepsilon = 1 \cdot 10^{-16}$			
	$\|e\|_\infty$	Rate	$\|e\|_{L_2}$	Rate	$\|e\|_\infty$	Rate	$\|e\|_{L_2}$	Rate
32	$1.272 \cdot 10^{-1}$	—	$1.049 \cdot 10^{-2}$	—	$1.272 \cdot 10^{-1}$	—	$8.558 \cdot 10^{-3}$	—
64	$6.054 \cdot 10^{-2}$	1.07	$3.256 \cdot 10^{-3}$	1.69	$6.053 \cdot 10^{-2}$	1.07	$2.140 \cdot 10^{-3}$	2.00
128	$2.143 \cdot 10^{-2}$	1.50	$1.029 \cdot 10^{-3}$	1.66	$2.143 \cdot 10^{-2}$	1.50	$5.350 \cdot 10^{-4}$	2.00
256	$7.280 \cdot 10^{-3}$	1.56	$3.215 \cdot 10^{-4}$	1.68	$7.280 \cdot 10^{-3}$	1.56	$1.338 \cdot 10^{-4}$	2.00
512	$2.321 \cdot 10^{-3}$	1.63	$9.899 \cdot 10^{-5}$	1.70	$2.321 \cdot 10^{-3}$	1.65	$3.344 \cdot 10^{-5}$	2.00

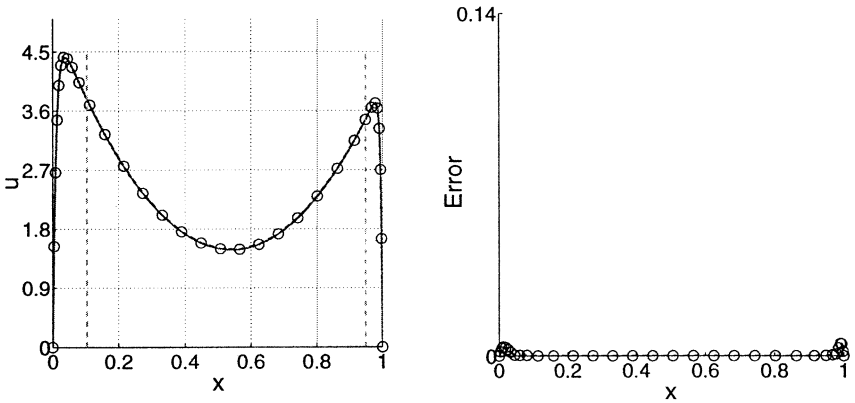

Fig. 5. Numerical solution and error using approximate equidistribution for Example 3 with $m = 3$, $N = 32$, and $\varepsilon = 1 \cdot 10^{-2}$.

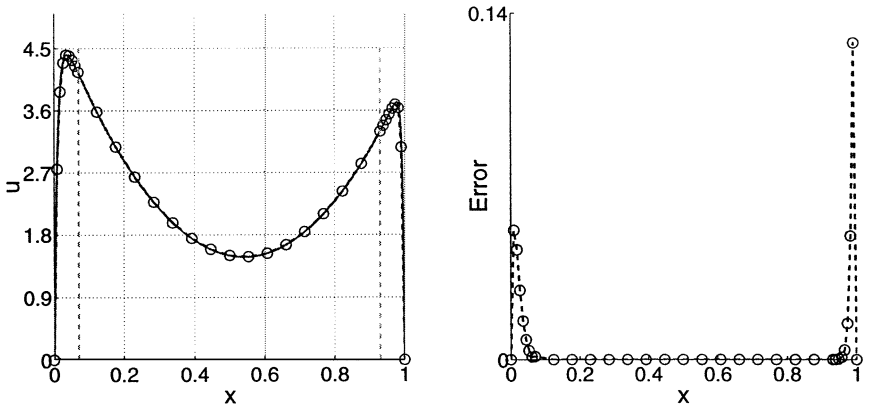

Fig. 6. Numerical solution and error using a Shishkin grid for Example 3 with $\tau_0 = 2$, $N = 32$, and $\varepsilon = 1 \cdot 10^{-2}$.

6. Conclusions

We have shown that the standard central difference approximation of a model singularly perturbed reaction–diffusion problem is uniformly accurate on a grid based on an equidistribution principle. The motivation for the analysis is to explain the observed behaviour of an adaptive solution procedure that does not require any a priori knowledge of the solution. We have proposed a monitor function that automatically detects the presence of boundary layers, their thickness, and their steepness. The equidistributed grid is exponentially stretched within the boundary layers and this is responsible for an improved rate of convergence compared to related piecewise uniform grids. The proposed monitor function has also been successfully used for singularly perturbed convection–diffusion problems, see [4].

The error analysis given in this paper is based on the assumption that the grid is given. It remains to analyse the fully adaptive system where the grid is determined from the numerical solution. Numerical experiments presented here suggest that the solutions obtained using a discretisation of the equidistribution principle are indeed ε-uniformly accurate and are very similar to those obtained on the analysed grids. Future research will also include an investigation of high-order discretisations, nonlinear problems, and the extension of the ideas given here to solve multi-dimensional boundary value problems.

Appendix

The aim of this appendix is to show that when the standard central difference scheme is applied to the solution of the constant coefficient version of (1) with $b(x)=\beta$ using a nonuniform grid based on the equidistribution of (8) with $m=4$, the truncation error in the singular component is fourth order. Using Taylor series expansions we have

$$\tau_j^W = \varepsilon \left\{ \sum_{n=2}^{\infty} \frac{w^{(n+1)}}{(n+1)!} \left[\frac{(x_{j+1}-x_j)^n - (-1)^n (x_j - x_{j-1})^n}{(x_{j+1}-x_{j-1})/2} \right] \right\}. \tag{A.1}$$

The first three terms of (A.1) are

$$\tfrac{1}{3} w_j'''(x_{j+1} - 2x_j + x_{j-1}), \quad n=2,$$

$$\tfrac{1}{12} w_j^{iv}((x_{j+1}-x_j)(x_j - x_{j-1}) + (x_{j+1} - 2x_j + x_{j-1})^2), \quad n=3,$$

$$\tfrac{1}{60} w_j^{v}(x_{j+1} - 2x_j + x_{j-1})((x_{j+1}-x_j)^2 + (x_j - x_{j-1})^2), \quad n=4.$$

Since the grid point $x_j = x(\xi_j)$ then to $O(N^{-6})$

$$(x_{j+1} - 2x_j + x_{j-1}) = \frac{1}{N^2} x_{\xi\xi} + \frac{1}{12N^4} x_{\xi\xi\xi\xi}$$

and

$$(x_{j+1}-x_j)(x_j - x_{j-1}) + (x_{j+1} - 2x_j + x_{j-1})^2 = \frac{1}{N^2}(x_\xi)^2 + \frac{1}{N^4}\left(\frac{1}{3} x_\xi x_{\xi\xi\xi} + \frac{3}{4}(x_{\xi\xi})^2\right).$$

Therefore,

$$\tau_j^W = \frac{\varepsilon}{N^2}\left[\frac{1}{3}w'''x_{\xi\xi} + \frac{1}{12}w^{\mathrm{iv}}(x_\xi)^2\right] + \mathrm{O}(\varepsilon N^{-4}).$$

The truncation error will be fourth order if $x(\xi)$ is chosen such that

$$\tfrac{1}{3}w'''x_{\xi\xi} + \tfrac{1}{12}w^{\mathrm{iv}}(x_\xi)^2 = 0.$$

Inside the two boundary layer regions this is equivalent to requiring

$$\frac{x_{\xi\xi}}{(x_\xi)^2} = -\frac{1}{4}\sqrt{\frac{\beta}{\varepsilon}}. \tag{A.2}$$

If we assume that $j \leqslant k_{l-1}$ and $m\sqrt{(\varepsilon/\beta)}\log(N) \ll 1$, then the grid points are approximately given by the mapping

$$\tilde{x}(\xi) = -m\sqrt{\frac{\varepsilon}{\beta}}\log\left(1 - \frac{2\xi}{\lambda_0}\right).$$

For this mapping we have

$$\tilde{x}_\xi = \sqrt{\frac{\varepsilon}{\beta}}\frac{2m}{(\lambda_0 - 2\xi)}, \quad \tilde{x}_{\xi\xi} = -\sqrt{\frac{\varepsilon}{\beta}}\frac{4m}{(\lambda_0 - 2\xi)^2}.$$

Hence, for (A.2) to be satisfied, we require $m = 4$. A similar argument establishes that the truncation error is fourth order when $j \geqslant k_r + 1$. To show that the truncation error in W is fourth order outside the boundary layer regions we simply apply Lemma 8 with $m = 4$.

References

[1] U.M. Ascher, R.M.M. Mattheij, R.D. Russell, Numerical Solution of Boundary Value Problems for Ordinary Differential Equations, Prentice-Hall, Englewood Cliffs, NJ, 1988.
[2] I. Babuška, W.C. Rheinbolt, A posteriori error estimates for the finite element method, Int. J. Numer. Methods Eng. 12 (1978) 1597–1615.
[3] A.S. Bakhvalov, On the optimization of methods for solving boundary value problems with boundary layers, J. Vychisl. Mat. i Mat. Fis. 9 (1969) 841–859.
[4] G. Beckett, J.A. Mackenzie, Convergence analysis of finite difference approximations on equidistributed grids for a singularly perturbed boundary value problem, Appl. Numer. Math., to appear.
[5] J.G. Blom, J.M. Sanz-Serna, J.G. Verwer, On simple moving grid methods for one-dimensional evolutionary partial differential equations, J. Comput. Phys. 74 (1988) 191–213.
[6] R.R. Brown, Numerical solution of boundary value problems using nonuniform grids, J. SIAM 10 (3) (1962) 475–495.
[7] C.J. Budd, H. Huang, R.D. Russell, Optimal meshes for a nearly singular boundary value problem, 1998, submitted for publication.
[8] G.F. Carey, H.T. Dinh, Grading functions and mesh redistribution, SIAM J. Numer. Anal. 22 (1985) 1028–1040.
[9] W.C. Connet, W.L. Golik, A.L. Schwartz, Superconvergent grids for two-point boundary value problems, Mathe. Appl. Comput. 10 (1991) 43–58.
[10] M. Dobrowolski, H.-G. Roos, A priori estimates for the solution of convection-diffusion problems and interpolation on Shishkin meshes, J. Anal. Appl. 4 (1997) 1001–1012.
[11] C. De Boor, Good approximation by splines with variables knots II, Lect. Notes Math. 363 (1974) 12–20.

[12] E.P. Doolan, J.J.H. Miller, W.H.A. Schilders, Uniform Numerical Methods for Problems with Initial and Boundary Layers, Boole Press, Dublin, 1980.
[13] B. Fornberg, A Practical Guide to Pseudospectral Methods, Cambridge University Press, Cambridge, 1996.
[14] E.G. Gartland, Graded-mesh difference schemes for singularly perturbed two-point boundary value problems, Math. Comp. 51 (1988) 631–657.
[15] W. Huang, D.M. Sloan, A simple adaptive grid method in two dimensions, SIAM. J. Sci. Comput. 15 (1994) 776–797.
[16] W. Huang, Y. Ren, R.D. Russell, Moving mesh PDEs based on the equidistribution principle, SIAM. J. Numer. Anal. 31 (1994) 709–730.
[17] J.A. Mackenzie, The efficient generation of simple two-dimensional adaptive grids, SIAM. J. Sci. Comput. 19 (1998) 1340–1365.
[18] J.A. Mackenzie, Uniform convergence analysis of an upwind finite-difference approximation of a convection–diffusion boundary value problem on an adaptive grid, IMA J. Numer. Anal. 19 (1999) 233–249.
[19] J.H.H. Miller, E. O'Riordan, G.I. Shishkin, Fitted Numerical Methods For Singular Perturbation Problems, World Scientific, Singapore, 1995.
[20] L.S. Mulholland, Y. Qiu, D.M. Sloan, Solution of evolutionary partial differential equations using adaptive finite differences with pseudospectral post-processing, J. Comput. Phys. 131 (1997) 280–298.
[21] E. O'Riordan, M. Stynes, A uniformly accurate finite element method for a singularly perturbed one-dimensional reaction–diffusion problem, Math. Comp. 47 (1986) 555–570.
[22] V. Pereyra, E.G. Sewell, Mesh selection for discrete solution of boundary problems in ordinary differential equations, Numer. Math. 23 (1975) 261–268.
[23] J.D. Pryce, On the convergence of iterated remeshing, IMA. J. Numer. Anal. 9 (1989) 315–335.
[24] Y. Qiu, D.M. Sloan, Analysis of difference approximations to a singularly perturbed two-point boundary value problem on an adaptively generated grid, J. Comput. Appl. Math. 101 (1999) 1–25.
[25] Y. Qiu, D.M. Sloan, T. Tang, Convergence analysis of an adaptive finite difference solution of a variable coefficient singular perturbation problem, 1996, submitted for publication.
[26] H.-J. Reinhardt, A posteriori error estimates for the finite element solution of a singularly perturbed linear ordinary differential equation, SIAM J. Numer. Anal. 28 (1981) 406–430.
[27] H.G. Roos, Global uniformly convergent schemes for a singularly perturbed boundary value problem using patched base spline-function, J. Comput. Appl. Math. 29 (1990) 69–77.
[28] R.D. Russell, J. Christiansen, Adaptive mesh selection strategies for boundary value problems, SIAM J. Numer. Anal. 15 (1978) 59–80.
[29] G.I. Shishkin, Difference schemes for singularly perturbed parabolic equation with discontinuous boundary condition, J. Vychisl. Mat. i Mat. Fis. 28 (1988) 1679–1692.
[30] R. Vulanović, Non-equidistant generalizations of the Gushchin–Schennikov scheme, ZAAM. 67 (1987) 625–635.
[31] A.B. White, On selection of equidistributing meshes for two-point boundary-value problems, SIAM J. Numer. Anal. 16 (1979) 472–502.